Supplementary Information (SI) for Energy & Environmental Science.
This journal is © The Royal Society of Chemistry 2024

Supplementary Information

Interlayer reinforcement for improved mechanical reliability for wearable perovskite solar cells

Weilun Cai[†1], Pengchen Zou[†2], Shiqi Rong[†3,4], Hui Wang[3], Xin Chen[1], Zheng zhang[1], Yajie Wang[1], Chou Liu[1], Tinghuan Yang[1], Tianqi Niu[1], Shengye Jin[3], Wenming Tian*[3], Jianxi Yao*[2], Shengzhong (Frank) Liu*[1,3], Kui Zhao*[1]

[1]*Key Laboratory of Applied Surface and Colloid Chemistry, Ministry of Education, Shaanxi Key Laboratory for Advanced Energy Devices, Shaanxi Engineering Lab for Advanced Energy Technology, School of Materials Science & Engineering, Shaanxi Normal University, Xi'an, P. R. China.*

[2]*State Key Laboratory of Alternate Electrical Power System with Renewable Energy Sources, Beijing Key Laboratory of Energy Safety and Clean Utilization, North China Electric Power University, Beijing, China.*

[3]*Key Laboratory of Photoelectric Conversion and Utilization of Solar Energy, Dalian Institute of Chemical Physics, Chinese Academy of Sciences, Dalian, 116023, Liaoning, China；Center of Materials Science and Optoelectronics Engineering, University of Chinese Academy of Sciences, Beijing, 100049, P. R. China.*

[4]*University of Chinese Academy of Sciences, Beijing 100049, China.*

† These authors contributed equally to this work.

**Email:tianwm@dicp.ac.cn; jianxiyao@ncepu.edu.cn; szliu@dicp.ac.cn; zhaok@snnu.edu.cn*

Experimental Section

Materials preparation: Polyacrylamide (PAM) was purchased from Acros. PET/ITO, Polyethylene terephthalate/indium tin oxide (PET/ITO), Methylammonium chloride (MACl, 98%) and formamidine iodide (FAI, 99.5%) were purchased from Advanced Election Technology Co., Ltd. Lead (II) iodide (PbI_2, 99.9%), Cesium iodide (CsI, 99.5%), Methylammonium iodide (MAI, 99.5%) and 2-Phenylethanamine hydroiodide (F-PEAI) were purchased from Xi'an Polymer Light Technology Cory. SnO_2 colloidal dispersion (15% in H_2O), Li-bis-(trifluoromethanesulfonyl) imide (Li-TFSI, ≥99%), 4-tert-butylpyridine (TBP, ≥96%), dimethyl sulfoxide (DMSO, 99.9%) and N, Ndimethylformamide (DMF, 99.8%) were obtained from Alfa Aesar. Were purchased from Advanced Election Technology Co., Ltd. Chlorobenzene (CB) and isopropanol (IPA) were purchased from China National Pharmaceutical Group Corporation. Anti-reflective layer was purchased from Liaoning Yike Precision New Energy Technology Co., Ltd.

Device fabrication: Device (0.09 cm^{-2}) fabrication: PET/ITO were cleaned with detergent solution (1:100), deionized water for 30 min for each step. The substrates were then treated by UV for 15 min to improve hydrophilicity. SnO_2 colloidal dispersion was diluted with deionized water (volume ratio, 1:6) SnO_2 was spin-coated on the PET/ITO substrate at 4000 rpm for 30 s. Finally, prepared PET/ITO/SnO_2 substrate was annealed at 100 °C for 60 min. For PAM modification, PAMs solution (0.3 mg mL^{-1} in deionized water) was spin-coated onto SnO_2 ETL at 4000 rpm for 30 s and annealed at 100 °C for 5 min in ambient air. The perovskite solution was prepared by dissolving 783 mg PbI_2, 269 mg FAI, 18 mg CsI, 11 mg MAI, 45 mg MACl and 57 mg $MAPbI_3$ in a mixed solvent of DMF and DMSO (volume ratio, 4:1). Before spin coting, the prepared SnO_2 substrate was treated with UV-Ozone for 12 min. Perovskite solution was spin-coated onto SnO_2 ETL at 6000 rpm for 30 s, followed by annealing at 120 °C for 20 min in ambient air (~40% humidity). PEAI solution (5 mg mL^{-1} in IPA) was spin-coated on the perovskite films, followed by 5 min annealing at 100 °C. Then the hole transport layer (HTL) was fabricated by spin coted 45 μL Spiro-OMeTAD solution (90 mg Spiro-OMeTAD, 36 μL TBP and 22 μL of Li-TFSI in 1 mL CB). The 80 nm gold electrode was deposited on the HTL. The anti-reflective lay was attached to the back of the substrate before *J–V* characteristics. Module (20 cm^{-2}) fabrication: ITO-coated and SnO_2-coated PEN substrates were covered with poly(tetrafluoroethylene) (PTFE) tape and placed in a chamber filled

with HCl vapor to selectively etch the unmasked area, forming P1lines with a width of 200 μm. For the blade-coated perovskite film, 45 μL of $FA_{0.95}Cs_{0.05}Pb(I_{0.95}Br_{0.05})_3$ precursor solution was drop-cast onto the 40 °C pre-heated SnO_2/FTO substrate at a speed of 1.5 m min^{-1}, and then annealed at 100 °C for 20 min. For HTL, 7 μL of Spiro-OMeTAD solution was dropped onto the 40 °C preheated substrate and blade-coated at a speed of 1 m min^{-1}. The 80 nm gold electrode was deposited on the HTL. P2 and P3 scribing lines were created using a 355 nm picosecond laser scriber (MM2500OpTek system, Inc., USA) with a laser power of 12 W and a pulse repetition rate of 100 kHz. The width of P2, etched with a laser power of 1.2 W and 70 kHz pulse repetition rate, was 100 μm. The 80 μm P3 gap was ablated using a 0.78 W laser power and 80 kHz pulse repetition rate. The distances between Pl and P2, as well as P2 and P3, were both 30 μm.

Device characterization: The photoluminescence (PL) and photocurrent mappings are performed on a home-built laser-scanned and time-resolved PL microscopy coupled with a photocurrent detection module. For PL measurements, a pulse laser (405 nm with 20 MHz repetition rate LDH-P-C-405, PicoQuant, Germany) is focused on the sample through a 100 X oil objective lens (NA = 1.4, Olympus UPlanSApo). The laser intensity at samples is adjusted by a neutral density filter and measured with a power meter (PM100D S130VC, Thorlabs, USA). The PL signal is collected by a high-speed detector (MPD, PicoQuant, Germany) with a 710 nm long-pass filter and the PL image is achieved by rotating the galvanometer mirror before the detector. To ensure that only PL from a diffraction-limited spot was observed, 100 μm pinhole size is chosen before the detector. For photocurrent measurements, a CW laser with wavelength of 405 nm (LDH-P-C-405, PicoQuant, Germany) is coupled to the system and the photocurrent is detected by using a Keithley 6485 picoammeter. The photocurrent image is obtained by scanning the laser spot and recording the photocurrent during scanning of each point on the perovskite solar cell. *J–V* characteristics of the devices were obtained using a Keithley 2400 Source Meter under ambient conditions(1.5 – –0.1 V, step: 0.02 V, delay time: 20 ms). The power of the lamp was calibrated using a National Renewable Energy Laboratory traceable KG5-filtered silicon reference cell. The external quantum efficiency was measured on a QE-R system (Enli Technology Co., Ltd.) using a 300-W Xe lamp as the light source. The monochromatic light intensity for EQE measurements was calibrated using a reference silicon photodiode.

Material characterization: Fourier transform infrared (FTIR) spectra were recorded with a Bruker VERTEX 70 infrared spectrophotometer using KBr sheets. Scanning electron microscopy (SEM) images were obtained using a Hitachi SU-8020 field-emission scanning electron microscope (Japan). Grazing incidence X-ray diffraction (GIXRD) and X-ray diffraction (XRD) studies were performed using a DX-2700BH diffractometer (Dandong Haoyuan Instrument Co., Ltd.). Nanoscratche test was obtained through Synton-MDP needle tip scratch measurements. Derjaguin-Muller-Toporov (DMT) modulus were recorded with a Bruker Dimension ICON. Grazing incidence wideangle scattering (GIWAXS, λ = 1.24 Å, incidence angle: 0.40°) was performed at the National Facility for Protein Science in Shanghai. The photoluminescence (PL) was performed on a home-built laser-scanned and time-resolved PL microscopy coupled with a photocurrent detection module. For PL measurements, a pulse laser (405 nm with 20 MHz repetition rate LDH-P-C-405, PicoQuant, Germany) is focused on the sample through a 100 X oil objective lens (NA = 1.4, Olympus UPlanSApo). The laser intensity at samples is adjusted by a neutral density filter and measured with a power meter (PM100D S130VC, Thorlabs, USA). The PL signal is collected by a high-speed detector (MPD, PicoQuant, Germany) with a 710 nm long-pass filter and the PL image is achieved by rotating the galvanometer mirror before the detector. To ensure that only PL from a diffraction-limited spot was observed, 100 μm pinhole size is chosen before the detector. The capacitance–voltage (C–V) measurements were performed on an electrochemical workstation (Modulab XM, USA) and the frequency was set to 200 kHz and the scan voltage range was 0–1.6 V. X-ray photoelectron spectroscopy (XPS) was performed on a photoelectron spectrometer (ESCALAB Xi+, Thermo Fisher Scientific). The film thickness was obtained through level gauge testing using a KLA-Tencor Alpha-stepD-600. UV-visible absorption spectra were acquired on a PerkinElmer UV Lambda 950 instrument. The in-situ crystallization process images were photographed by an optical microscopy (BX53M, Olympus, Japan). The as-prepared perovskite wet films were transferred to a hot plate at 60° and subsequently photographed using microscope to record the crystallization process.

Bending durability tests: The bending durability of F-PSCs was evaluated using a mechanical tester (Prtronic, FT2000) in constant-radius bending mode with a bending radius of 7 mm in ambient air.

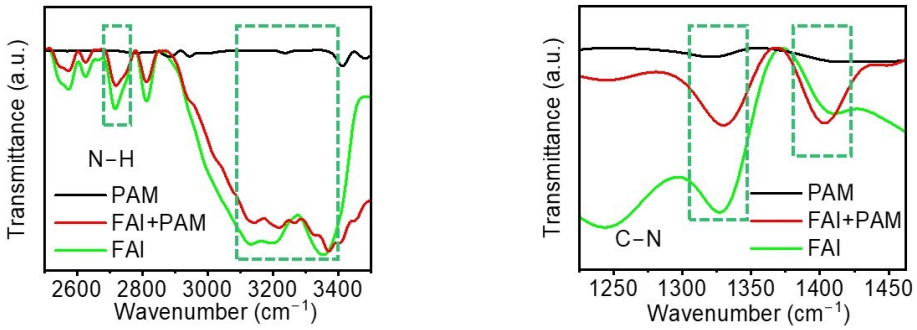

Figure S1. FTIR spectra of PAM+FAI compounds.

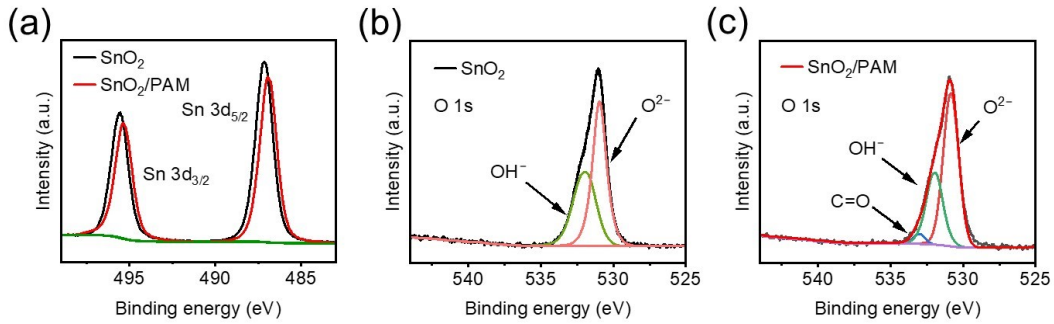

Figure S2. XPS spectra of SnO_2 and PAM+SnO_2 **(a)** Sn $3d_{3/2}$ **(b), (c)** O 1s.

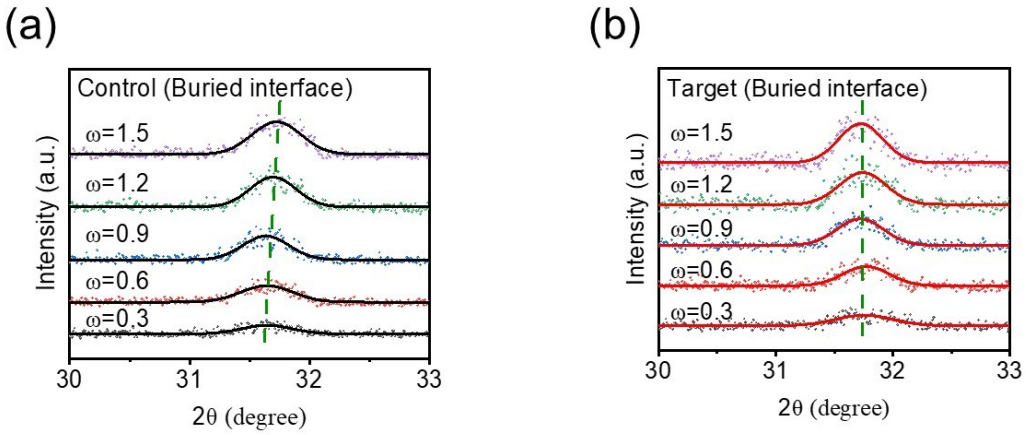

Figure S3. GIXRD spectra of **(a)** control (buried interface) and **(b)** target (buried interface).

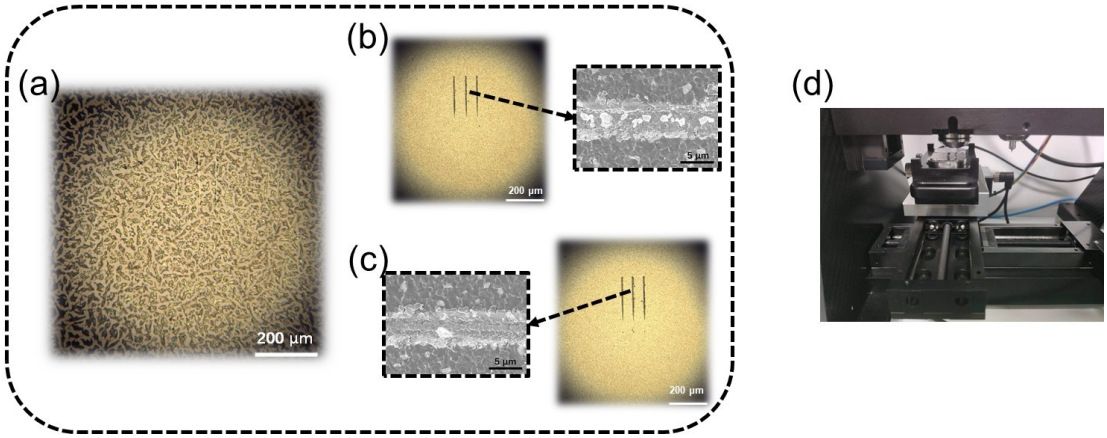

Figure S4. Nanoscratch tests on three interfaces.

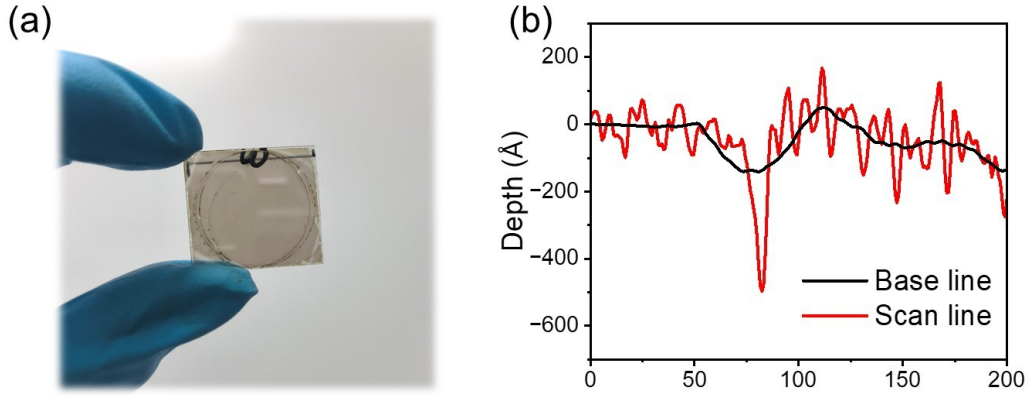

Figure S5. (a) The perovskite film of 50 nm, **(b)** data of the step gauge.

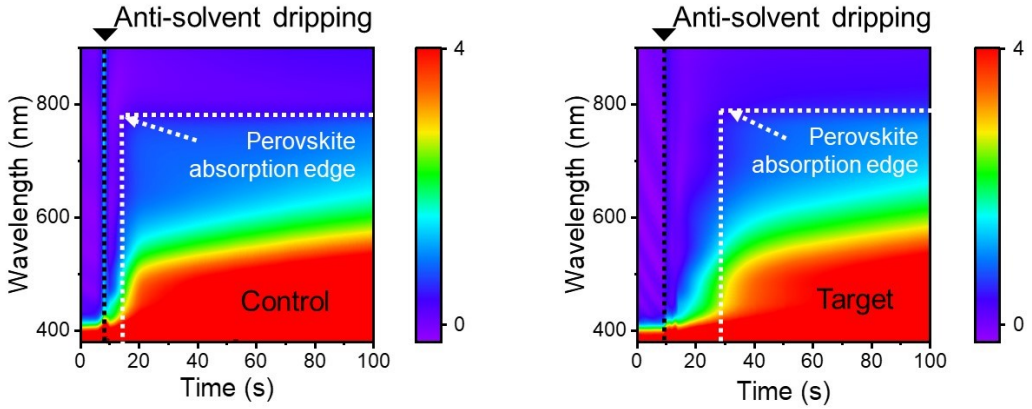

Figure S6. The UV-visible absorption spectroscopy of spin-coating.

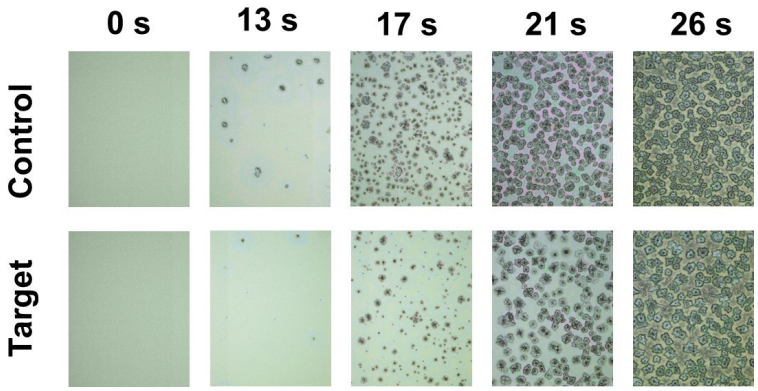

Figure S7. The optical microscopy of perovskite film.

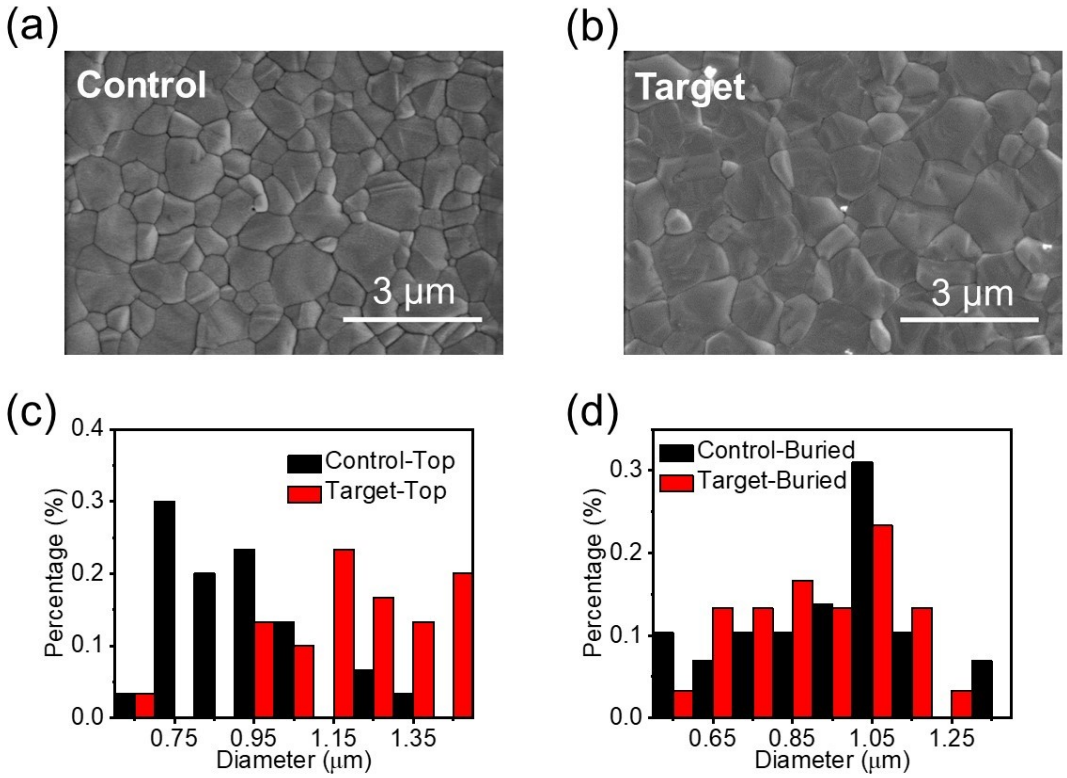

Figure S8. SEM images **(a, b)**, and the corresponding grain size distributions **(c, d)** of the perovskite films with PAM and without PAM, respectively.

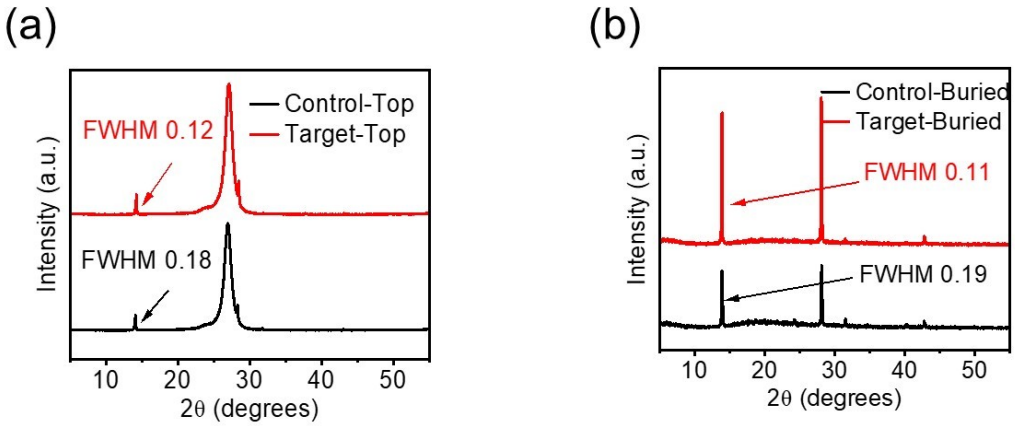

Figure S9. XRD spectra of top interface and buried interface.

PHOTOVOLTAIC AND WIND POWER SYSTEMS QUALITY TEST CENTER, IEE, CHINESE ACADEMY OF SCIENCES

Report No: PWQC-WT-P23110721-1R

Sample code	DC2023a102
Sample S/N	1
Type	Single Junction Flexible Perovskite Solar Cell
Designated area	0.0624 cm^2 The designated area was offered by the client.

Items of testing	Measurement of photovoltaic current-voltage characteristics				
Sample code	DC2023a102				
Results	**Isc** (mA)	**Jsc** (mA/ cm^2)	**Voc** (V)	**Pm** (mW)	**Curve**
	1.602	25.667	1.183	1.523	A202311071 12842
	Ipm (mA)	**Vpm** (V)	**FF** (%)	**E_{ff}** (%)	
	1.523	1.000	80.38	24.41	

Measurement uncertainty:

$U_{95(Isc)}$=1.9% (k=2)

$U_{95(Voc)}$=1.8% (k=2)

$U_{95(Pm)}$=2.5% (k=2)

Figure S10. Certification of the target device at the IEE, Chinese academy of sciences, China. The PCE is 24.4% (V_{OC} = 1.183 V, I_{SC} = 1.602 mA, FF = 80.38%).

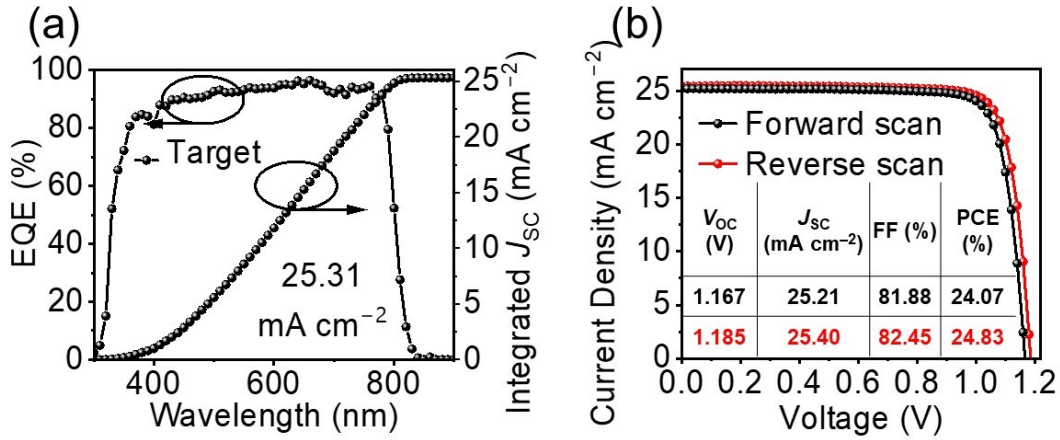

Figure S11. (a) EQE curves and integrated current densities, **(b)** The forward and reverse scan J-V curves of the target device.

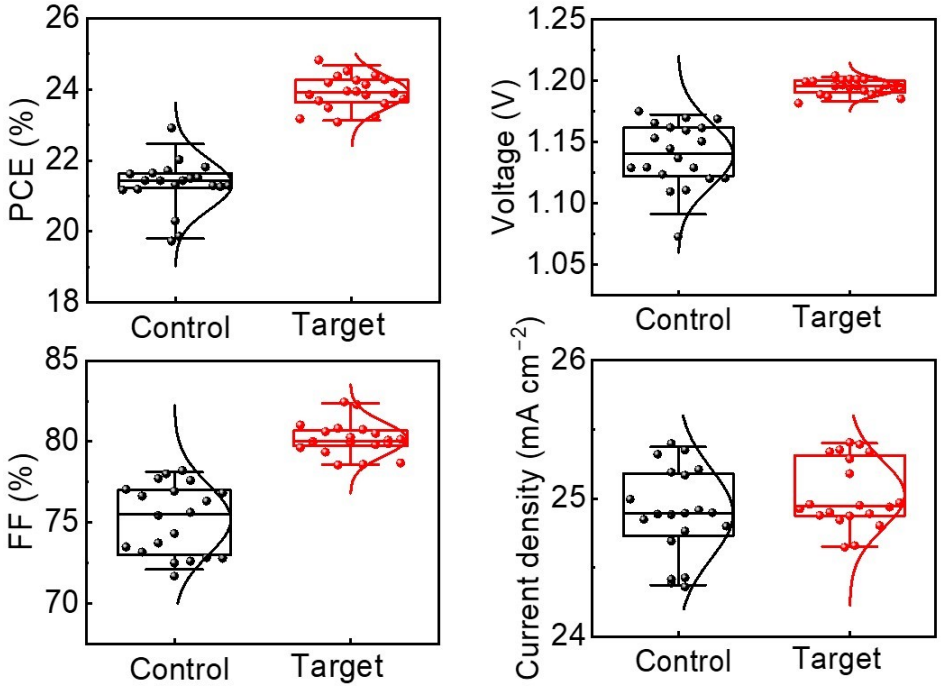

Figure S12. Statistical comparison of *J-V* parameters of control and target devices.

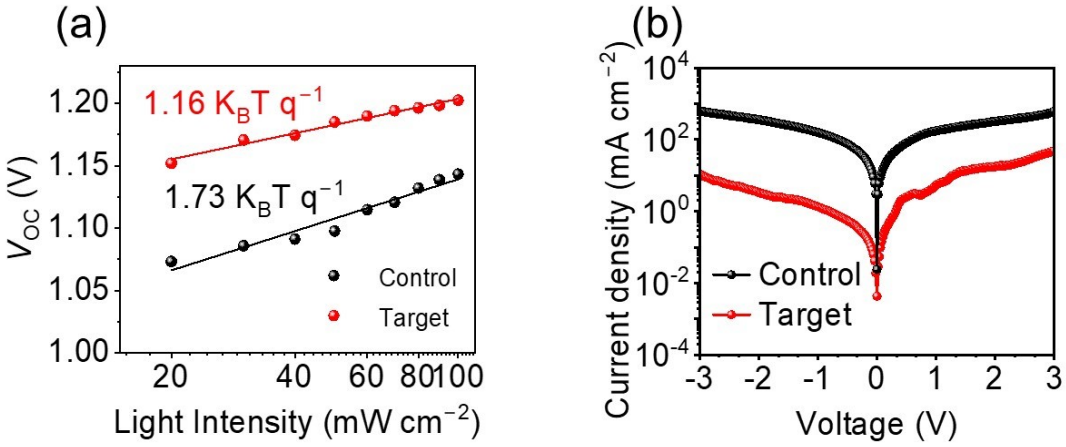

Figure S13. (a) Open-circuit voltage versus sunlight intensity, **(b)** Dark *J-V* curves.

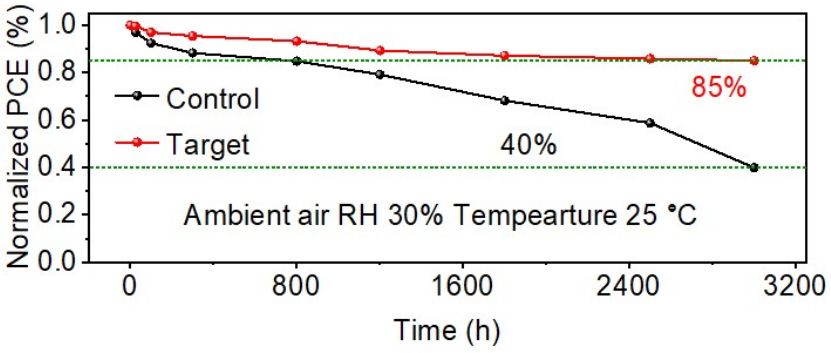

Figure S14. PCE evolution observed for the control and target devices stored without encapsulation at ambient conditions (25 °C and 30–40% relative humidity).

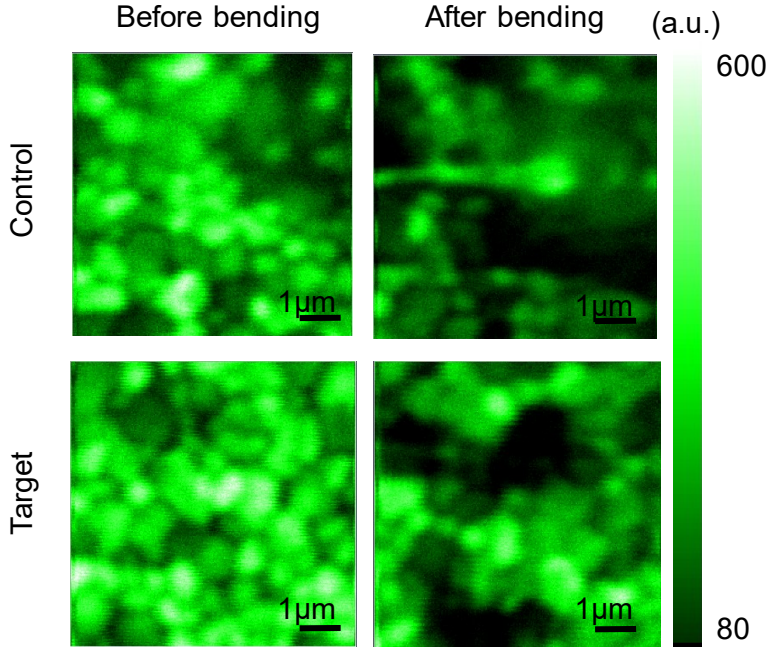

Figure S15. PL mappings on working flexible devices (before and after bending).

Table S1 Statistics of nanoscratch tests on three interfaces.

Parameters	1 (mN)	2 (mN)	3 (mN)	Average (mN)	Absolute error (mN)	Relative deviation
SnO_2/perovskite	1.256	1.511	1.260	1.342	0.112	8.371%
SnO_2/PAM	5.214	3.249	5.177	4.546	0.865	19.035%
PAM/perovskite	6.474	8.694	5.239	6.802	1.261	18.539%

Table S2 The summary of device parameters for the state-of-the-art small-area F-PSCs.

Years	PCE (%)	Certified PCE (%)	References
2022	22.1	22.1	58
2022	20.86	/	59
2022	23.6	/	60
2022	20.2	/	61
2023	22.04	/	62
2023	23.86	/	63
2023	23.94	23.57	64
2023	23.4	22.9	65
2023	23.84	/	66

2023	22.3	/	55
2023	23.4	/	2
2023	23.68	23.35	67
2024	23.4	/	68
2024	23.48	/	69
2024	24.84	/	70
2024	23.52	/	71
2024	24.61	23.51	72
2024	24.9	24.48	28
2024	24.51	24.04	73
2024	22.61	/	74
2024	23.59	/	75
2024	25.09	24.9	76
2024	23.59	/	77
2024	22.8	/	78
2024	25.05	/	79
2024	23.02	/	80
2024	22.61	/	81

2024	24.47	/	82
This work	**24.83**	**24.41**	